

RESEARCH

Open Access



Identification of key transcription factors, including *DAL80* and *CRZ1*, involved in heat and ethanol tolerance in *Saccharomyces cerevisiae*

Rong-Rong Chen^{1,2}, Li Wang¹, Xue-Xue Ji^{1,2}, Cai-Yun Xie^{1,3*} and Yue-Qin Tang^{1,2}

Abstract

Background High temperature and ethanol are two critical stress factors that significantly challenge bioethanol production using *Saccharomyces cerevisiae*. In this study, the tolerance mechanisms of the multi-tolerant *S. cerevisiae* strain E-158 to heat stress and combined heat-ethanol stress were investigated using comparative transcriptomics.

Results Under heat stress at 44 °C, glucose transport and reactive oxygen species (ROS) scavenging were significantly upregulated, while gluconeogenesis, acetate formation, and dNDP formation showed significant downregulation. Under combined heat (43 °C) and ethanol (3% v/v) stress, glucose transport, glycolysis, acetate formation, peroxisome activity, ROS scavenging, and ribosome synthesis were significantly upregulated, while glycerol formation, cellular respiration and dNDP formation exhibited significant downregulation. Fourteen transcription factors (TFs), considered to play a key role in both stress conditions, were individually overexpressed and deleted in *S. cerevisiae* strain KF-7 in this study. Among these TFs, Gis1p, Crz1p, Tos8p, Yap1p, Dal80p, Uga3p, Mig1p, and Opi1p were found to contribute to enhanced heat tolerance in *S. cerevisiae*. Compared with KF-7, strains overexpressing *DAL80* and *CRZ1* demonstrated markedly improved fermentation performance under stress conditions. Under heat stress at 44 °C, glucose consumption increased by 10% and 12%, respectively, for strains KF7DAL80 and KF7CRZ1, while ethanol production increased by 12% and 15%, respectively, compared to KF-7. Under combined stress conditions of 43 °C and 3% (v/v) ethanol, glucose consumption increased by 67% and 44%, ethanol production by 116% and 77%, and ethanol yield by 29% and 22%, respectively, for KF7DAL80 and KF7CRZ1 compared to KF-7. KF7CRZ1 performs comparably to E-158, while KF7DAL80 outperforms E-158.

Conclusions This study provides valuable theoretical insights and identifies critical TF targets, contributing to the development of robust *S. cerevisiae* strains for improved bioethanol production.

Keywords *Saccharomyces cerevisiae*, Comparative transcriptome, Heat tolerance, Combined heat and ethanol stress, Transcription factors

*Correspondence:

Cai-Yun Xie

xiocy@scu.edu.cn

Full list of author information is available at the end of the article



© The Author(s) 2025. **Open Access** This article is licensed under a Creative Commons Attribution-NonCommercial-NoDerivatives 4.0 International License, which permits any non-commercial use, sharing, distribution and reproduction in any medium or format, as long as you give appropriate credit to the original author(s) and the source, provide a link to the Creative Commons licence, and indicate if you modified the licensed material. You do not have permission under this licence to share adapted material derived from this article or parts of it. The images or other third party material in this article are included in the article's Creative Commons licence, unless indicated otherwise in a credit line to the material. If material is not included in the article's Creative Commons licence and your intended use is not permitted by statutory regulation or exceeds the permitted use, you will need to obtain permission directly from the copyright holder. To view a copy of this licence, visit <http://creativecommons.org/licenses/by-nc-nd/4.0/>.

Background

Bioethanol, characterized by its transportability, high energy density, and low greenhouse gas emissions, is considered a highly promising liquid fuel for low-carbon transportation [1]. *Saccharomyces cerevisiae*, known for its excellent ethanol production capacity and good tolerance to various stresses, has traditionally been the preferred strain for fuel ethanol production [2]. However, in industrial ethanol production, yeast cells face multiple stresses, such as high temperatures and elevated ethanol concentrations [3, 4]. These stress conditions can inhibit yeast growth, causing delays or complete stalls in fermentation, thereby significantly hindering industrial productivity. Moreover, to save time and reduce costs in the production of ethanol from lignocellulosic and starch-based feedstocks, the industry commonly employs simultaneous saccharification and fermentation (SSF) [5, 6]. There is a significant difference between the optimal temperature for enzymatic hydrolysis (45–50 °C) and that for fermentation (30–35 °C), leading to increased enzyme usage and higher cooling costs. Enhancing the growth and fermentation performance of *S. cerevisiae* under high-temperature conditions would, therefore, greatly benefit the SSF process. While *S. cerevisiae* has evolved certain mechanisms to tolerate individual stress, enhancing its tolerance to multiple concurrent stresses remains a critical challenge in industrial applications [7, 8]. Addressing this issue could significantly enhance the efficiency and cost-effectiveness of bioethanol production processes.

Several studies have attempted to isolate strains with thermotolerance from natural environments. Pandey et al. [9] isolated a *S. cerevisiae* strain, NGY10, from sugarcane distillery waste, which produced 46.81 g/L of ethanol during fermentation at 40 °C with an initial glucose concentration of 100 g/L. Auesukaree et al. [10] isolated a thermotolerant *S. cerevisiae* strain from tropical fruits that produced 38 g/L of ethanol under fermentation conditions of 41 °C and an initial glucose concentration of 100 g/L. Despite these achievements, pursuing higher thermal tolerance remains crucial for ensuring enzymatic activity and fermentation efficiency. Therefore, further improving the high-temperature tolerance of cells is indispensable.

To identify potential targets for improving tolerance, many researchers have employed omics technologies to elucidate the stress–response mechanisms of *S. cerevisiae* strains to high temperatures, ethanol, and other stresses. Yang et al. [11] obtained an ethanol-tolerant mutant, YN81, using ultraviolet–diethyl sulfate (UV–DES) mutagenesis. Through comparative transcriptomics, they highlighted the importance of membrane-associated genes for ethanol tolerance. Gan et al. [12] knocked out

23 transcription factors (TFs) and identified three key TFs associated with thermotolerance: Sin3p, Srb2p, and Mig1p. However, current research still has limitations. Many studies have focused on single-stress conditions, whereas fermentation processes typically involve multiple concurrent stresses. Furthermore, the strains used in these studies often have weak inherent tolerance to stresses, including ethanol, heat, and toxic inhibitors, which makes their response mechanisms and gene targets less relevant for practical applications. Understanding the response mechanisms of multi-stress-tolerant *S. cerevisiae* strains under multiple stress conditions would provide more valuable guidance for constructing robust strains suitable for industrial production.

In our earlier work, a multi-tolerant industrial *S. cerevisiae* strain, E-158, was developed [13]. E-158 exhibited superior tolerance to five stress conditions: high temperature, high ethanol concentration, combined heat and ethanol stress, high sugar concentration, and high salt concentration [13]. A comparative transcriptome analysis of strain E-158 and its original strain, KF-7, under five stress conditions identified 28 shared differentially expressed genes (DEGs) [14]. The overexpression of *CRZ1* and *ENA5*, along with the deletions of *ASP3*, *YOL162W*, *YOR012W*, and *TOS8* in strain KF-7, was found to significantly enhance tolerance to multiple stress conditions [14]. In the present study, a detailed comparative transcriptome analysis was performed under two stress conditions: high temperature (44 °C) and combined heat-ethanol stress (43 °C and 3% v/v ethanol). The study aims to identify key TFs involved in thermotolerance and dual-stress tolerance to heat and ethanol. These findings provide valuable theoretical insights and offer promising targets for the development of robust strains specifically tailored for industrial bioethanol production.

Methods

Strains and media

All strains used in this study are listed in Table 1. The flocculating diploid industrial *S. cerevisiae* strain KF-7 was used as the original strain [15]. The multi-tolerant strain E-158 was derived from KF-7 [13]. *E. coli* DH5 α (Takara Bio Inc., Japan) was used for gene cloning and manipulation.

YP medium (10 g/L yeast extract and 20 g/L peptone) containing 20 g/L glucose (YPD20) was used for the routine cultivation of yeast cells. YPD20 agar plates were used for cell activation. YP medium containing 50 g/L glucose (YPD50) was used for pre-cultivation. YP medium with 150 g/L glucose (YPD150) was used for fermentation under heat stress, while YP medium with 100 g/L glucose and 3% (v/v) ethanol (YPDE100) was used for fermentation under combined heat-ethanol stress. YPD agar plates

Table 1 *Saccharomyces cerevisiae* strains used in this study

Strains	Description	References
KF-7	<i>MATa/a, Flo⁺, Spo⁻</i>	[15]
E-158	KF-7, Random mutagenesis and hybridization	[13]
KF7ΔYAP1	KF-7, <i>Δyap1</i>	This study
KF7ΔRPH1	KF-7, <i>Δrph1</i>	This study
KF7ΔCRZ1	KF-7, <i>Δcrz1</i>	This study
KF7ΔGIS1	KF-7, <i>Δgis1</i>	This study
KF7ΔPUT3	KF-7, <i>Δput3</i>	This study
KF7ΔMIG1	KF-7, <i>Δmig1</i>	This study
KF7ΔPHD1	KF-7, <i>Δphd1</i>	This study
KF7ΔOP11	KF-7, <i>Δrph1</i>	This study
KF7ΔYJL206C	KF-7, <i>Δyjl206c</i>	This study
KF7ΔDAL80	KF-7, <i>Δdal80</i>	This study
KF7ΔUGA3	KF-7, <i>Δuga3</i>	This study
KF7ΔIME1	KF-7, <i>Δime1</i>	This study
KF7ΔTOS8	KF-7, <i>Δtos8</i>	This study
KF7YAP1	KF-7, Replacement of promoter P _{YAP1} to P _{HHF2}	This study
KF7RPH1	KF-7, Replacement of promoter P _{RPH1} to P _{HHF2}	This study
KF7CRZ1	KF-7, Replacement of promoter P _{CRZ1} to P _{HHF2}	This study
KF7GIS1	KF-7, Replacement of promoter P _{GIS1} to P _{HHF2}	This study
KF7PUT3	KF-7, Replacement of promoter P _{PUT3} to P _{HHF2}	This study
KF7MIG1	KF-7, Replacement of promoter P _{MIG1} to P _{HHF2}	This study
KF7PHD1	KF-7, Replacement of promoter P _{PHD1} to P _{HHF2}	This study
KF7OP11	KF-7, Replacement of promoter P _{OP11} to P _{HHF2}	This study
KF7YJL206C	KF-7, Replacement of promoter P _{YJL206C} to P _{HHF2}	This study
KF7DAL80	KF-7, Replacement of promoter P _{DAL80} to P _{HHF2}	This study
KF7UGA3	KF-7, Replacement of promoter P _{UGA3} to P _{HHF2}	This study
KF7IME1	KF-7, Replacement of promoter P _{IME1} to P _{HHF2}	This study
KF7TOS8	KF-7, Replacement of promoter P _{TOS8} to P _{HHF2}	This study
KF7IFH1	KF-7, Replacement of promoter P _{IFH1} to P _{HHF2}	This study

supplemented with 100 µg/mL geneticin (G418), 50 µg/mL nourseothricin (NAT), or both, were used to select yeast transformants. All YP media were maintained at their natural pH without adjustment. Luria Bertani (LB) medium (5 g/L yeast extract, 10 g/L peptone, 10 g/L NaCl, pH 7.0) supplemented with 100 µg/mL ampicillin (Amp), 100 µg/

mL kanamycin (Kan), or 50 µg/mL nourseothricin (NAT) was used to select *E. coli* transformants.

Transcriptomic data analysis

In the preliminary study, RNA sequencing was conducted on strains E-158 and KF-7 under two stress conditions: a high temperature of 44 °C and a combined heat-ethanol stress at 43 °C with 3% (v/v) ethanol [14]. For RNA extraction, cells were harvested at 16 h of fermentation under 44 °C and at 12 h under the condition of 43 °C with 3% (v/v) ethanol. Total RNA was extracted using the Yeast RNA Kit (Omega Bio-Tek, USA), adhering to the manufacturer's guidelines. RNA degradation and contamination were monitored through agarose gel electrophoresis. The concentration and purity of the RNA were assessed using Nanodrop2000 (Implen, CA, USA), while its integrity was evaluated by Agilent 5300 (with RQN > 6.5). The RNA-seq library preparation and sequencing were carried out on an Illumina Novaseq 6000 platform by Shanghai Majorbio Biopharm Technology Co. Ltd. (Shanghai, China). After filtering the raw sequencing data, high-quality sequencing data (clean data) were obtained.

The comparative transcriptome analysis was conducted as previously described by Wang et al. [14]. Gene function annotations were obtained from the *Saccharomyces* Genome Database (SGD, <https://www.yeastgenome.org/>). Gene expression levels were estimated using transcripts per million (TPM). Differential expression analysis was performed using the DESeq2 software. Genes with a false discovery rate (FDR) < 0.05 and an absolute fold change (FC) ≥ 1.5 were identified as differentially expressed genes (DEGs). Kyoto Encyclopedia of Genes and Genomes (KEGG) enrichment analysis of the DEGs was performed using the KEGG database (<http://www.genome.jp/kegg/>). KEGG pathways with a $p_{\text{adj}} < 0.05$ and enrichment ratio > 0.01 were considered to be significantly enriched. The enrichment ratio of each KEGG pathway was the number of DEGs involved in each pathway to the number of total DEGs. Transcription factor (TF) analysis was performed using the YEASTRACT database (<http://www.yeasttract.com/>) based on DEGs with an absolute FC ≥ 2. TFs with an absolute FC ≥ 1.5 were identified as significantly differentially expressed transcription factors (DETFs). The interactions among all DETFs were analyzed, and the regulatory ratio of a given DETF (X) to other DETFs was calculated using the following formula:

$$\text{Regulatory ratio of X} = \left(\frac{\text{Number of DETFs regulated by X}}{\text{Total number of DETFs}} \right) \times 100\%.$$

DETFs with a regulatory ratio exceeding 25% were considered central nodes. Furthermore, the consistency ratio

of expression between a given DETF (X) and its targeting DEGs was calculated using the following formula:

$$\text{Consistency ratio of X} = \left(\frac{\text{Number of DEGs activated by X while showing consistent expression trends with X} + \text{Number of DEGs repressed by X while showing opposite expression trends to X}}{\text{Total number of DEGs regulated by X}} \right) \times 100\%.$$

gRNA plasmid construction

Details of the plasmids used in this study are provided in Table 2, while the primers are listed in Additional file 2: Table S1. A specific guide RNA (gRNA) sequence for each gene was designed using the CRISPOR tool (<https://crispor.gi.ucsc.edu/>) [16], and primers designated as XX_gF, incorporating these gRNA sequences, were subsequently synthesized. For the construction of the gRNA plasmids, linearized plasmid backbones were amplified from the pMEL13 plasmid using phosphorylated primers gRNA_R and XX_gF. The resulting PCR products underwent self-ligation to form the gRNA plasmids. All sequences were confirmed by sequencing.

Repair fragment preparation

To achieve gene overexpression, the native promoters of the target genes were replaced with the *HHF2* promoter. This promoter maintained moderate strength and stability under all tested stress conditions, as detailed in Additional file 2: Table S2. The *HHF2* promoter was amplified from the KF-7 genome using primers HHF2_F and HHF2_R and was integrated into the pMD19-T vector to generate plasmid pMD19-HHF2p. Subsequently, the

repair fragment for overexpression was amplified using pMD19-HHF2p as the template with primers XX_RF_F2

and XX_RF_R2. This fragment comprised the *HHF2* promoter sequence (Additional file 2: Table S3), along with the upstream and downstream homologous arms of the target genes. For gene deletion, primers XX_RF_F and XX_RF_R were used to anneal and form double-stranded repair fragments. These fragments consisted solely of the upstream and downstream homologous arm of the target genes.

Strain construction

Genes were individually overexpressed or deleted using the CRISPR/Cas9 editing system. Yeast transformation was performed using the lithium acetate method as previously described [17]. First, the Cas9-NAT plasmid was introduced into KF-7 to generate KF7Cas9. Subsequently, gRNA plasmids and corresponding repair fragments were co-transformed into KF7Cas9. Transformants were selected on YPD agar plates supplemented with 100 µg/mL G418 and 50 µg/mL NAT. Successful integration was confirmed by colony PCR and Sanger sequencing. Correct transformants were then cultured in YPD media to eliminate the Cas9-NAT and gRNA plasmids according to Mans' method [18].

Table 2 Plasmids used in this study

Plasmids	Description	References
Cas9-NAT	<i>Amp^R</i> , <i>NAT</i> , <i>Cas9</i>	[18]
pMEL13	2 µm, <i>amp^R</i> , <i>KanMX</i> , <i>gRNA-CAN1.Y</i>	[18]
pMD19-T	2 µm, <i>amp^R</i>	TaKaRa Bio Inc
pMD19-HHF2p	pMD19-T, <i>HHF2</i> promoter	This study
pMEL13-YAP1	pMEL13, <i>gRNA-YAP1</i>	This study
pMEL13-RPH1	pMEL13, <i>gRNA-RPH1</i>	This study
pMEL13-CRZ1	pMEL13, <i>gRNA-CRZ1</i>	This study
pMEL13-GIS1	pMEL13, <i>gRNA-GIS1</i>	This study
pMEL13-PUT3	pMEL13, <i>gRNA-PUT3</i>	This study
pMEL13-MIG1	pMEL13, <i>gRNA-MIG1</i>	This study
pMEL13-PHD1	pMEL13, <i>gRNA-PHD1</i>	This study
pMEL13-OPI1	pMEL13, <i>gRNA-OPI1</i>	This study
pMEL13-YJL206C	pMEL13, <i>gRNA-YJL206C</i>	This study
pMEL13-DAL80	pMEL13, <i>gRNA-DAL80</i>	This study
pMEL13-UGA3	pMEL13, <i>gRNA-UGA3</i>	This study
pMEL13-IME1	pMEL13, <i>gRNA-IME1</i>	This study
pMEL13-TOS8	pMEL13, <i>gRNA-TOS8</i>	This study

Batch fermentation and analytical methods

Yeast cells were activated overnight on YPD20 agar plates at 30 °C and then pre-cultivated in 500 mL Erlenmeyer flasks containing 100 mL of YPD50 medium for 16 h. After pre-cultivation, the cells were collected and inoculated into 300 mL flasks containing 100 mL of fermentation media, with an initial cell density of 0.5 g dry cell weight (DCW)/L. The flasks were incubated in a thermostatically controlled water bath and stirred at 200 rpm for 48 h. To test the strains' performance under heat stress, fermentations were conducted using YPD150 at 43 °C and 44 °C, respectively. For the combined heat-ethanol stress condition, YPDE100 was used. Due to the synergistic effects of high temperature and ethanol causing more severe cellular inhibition than high temperature alone, fermentation was conducted at 43 °C to ensure sufficient activity. All fermentation experiments were performed independently in triplicate.

The fermentation broth was centrifuged, and the supernatant was filtered through a 0.22 µm membrane filter for

the determination of glucose, glycerol, and ethanol concentrations. Glucose and glycerol concentrations were determined by HPLC (LC-10 ADV, Shimadzu, Kyoto, Japan) at 25 °C, with a mobile phase of 5 mmol/L sulfuric acid at a flow rate of 0.6 mL/min. Ethanol concentration was determined using gas chromatography (GC 2010 Pro, Shimadzu, Japan). DCW was measured according to a previously published method [19]. All data represent the averages of triplicate experiments, with standard deviations provided. Statistical significance was determined using an independent samples *t* test.

Results

Mechanisms of tolerance to heat stress in strain E-158

Under heat stress at 44 °C, using a YP medium with 100 g/L glucose, strain E-158 exhibited a 31% increase in glucose consumption and a 33% increase in ethanol production compared to KF-7 [13]. A comparative transcriptomic analysis between E-158 and KF-7 identified 870 DEGs, of which 468 were upregulated and 402 were downregulated. All DEGs were subjected to KEGG pathway enrichment analysis (Fig. 1a, Additional file 2: Table S4).

Compared to KF-7, strain E-158 exhibited significant regulation of genes related to central carbon metabolism. Genes encoding hexose transporters (*HXT2*, *HXT8*, *HXT10*, *HXT13*, *HXT14*, *HXT15*, and *HXT17*) were upregulated, particularly those for high-affinity glucose transporters (*HXT2*, *HXT8*, *HXT10*, and *HXT14*). This upregulation likely contributes to the increased glucose consumption observed in E-158. Several genes involved in gluconeogenesis (*MDH2*, *PYCI*, and *PCK1*) and the glyoxylate cycle (*CIT2* and *IDP2*) were significantly downregulated. In addition, *ALD4* and *ACS1* were also downregulated. The downregulation of these genes suggests that E-158 may inhibit pathways associated with the metabolism of non-fermentable carbon sources. Reduced expression of *ALD4* and *ACS1* has also been reported to promote the conversion of acetaldehyde to ethanol and minimize the production of toxic by-products like acetate [20]. Consequently, E-158 showed enhanced glucose transport and suppressed non-fermentable carbon source metabolism, reducing the synthesis of toxic by-products such as acetate. This metabolic reprogramming probably plays a role in enhancing the thermotolerance of E-158.

In cellular redox processes, several genes are involved in the scavenging of reactive oxygen species (ROS), including those encoding superoxide dismutase (*SOD2*), cytoplasmic catalase (*CTT1*), methionine-S-sulfoxide reductase (*MXR1*), and glutathione peroxidase (*GPX1*). Research has shown that *SOD2* plays a protective role in thermotolerance, and its deletion leads to increased sensitivity to high temperature [21]. Overexpression of

CTT1 has been demonstrated to significantly reduce lipid peroxidation and delay apoptosis induction under stress conditions [22]. In addition, the glutathione system and thioredoxin system contribute to rapid ROS clearance from cells. These genes were upregulated in E-158, suggesting that enhanced ROS scavenging capacity may be a key factor in the improved thermotolerance of E-158.

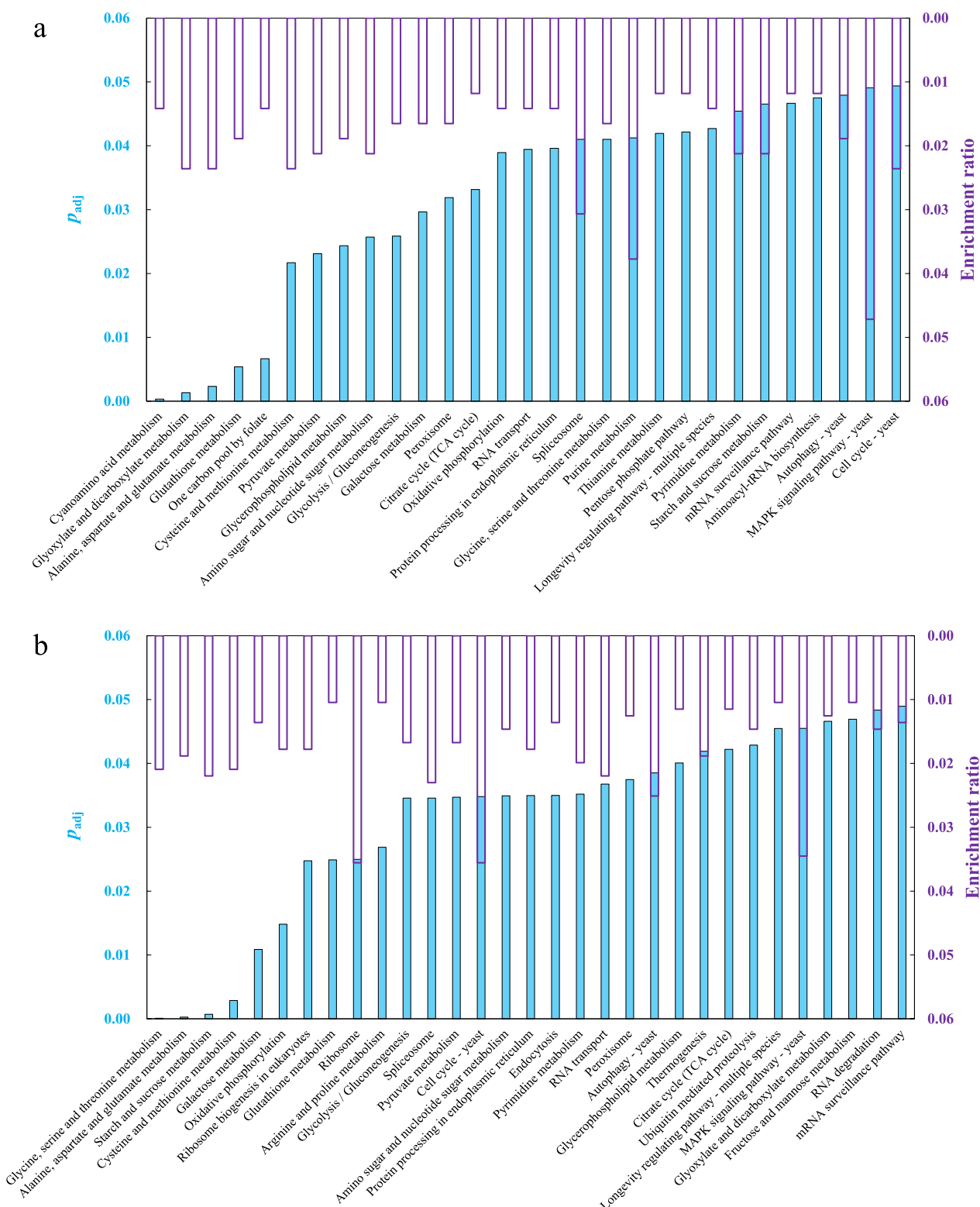
It was observed that under heat stress, the genes *RNR1*, *RNR2*, *RNR3*, and *RNR4*, which encode the subunits of ribonucleotide-diphosphate reductase (RNR), were all downregulated in E-158. The RNR complex catalyzes the reduction of ribonucleotide diphosphates (NDPs) to deoxyribonucleotide diphosphates (dNDPs), a process that constitutes the rate-limiting step in DNA synthesis [23]. This reaction also requires reducing equivalents such as NADPH [24]. Therefore, while the downregulation of RNR-associated genes under heat stress may limit the synthesis of dNDP, it could also lead to a redirection of reducing power, like NADPH, toward antioxidant protection. This metabolic adjustment might serve as an adaptive strategy, allowing cells to allocate more resources to combating oxidative stress induced by heat.

In summary, compared to strain KF-7, strain E-158 exhibits a multifaceted adaptive response to cope with heat stress at 44 °C. This response includes enhancing glucose uptake, inhibiting the metabolism of non-fermentable carbon sources, reducing acetate formation, increasing the capacity to clear ROS, reducing the synthesis of dNTPs, and redirecting more reducing equivalents toward antioxidant defenses (Fig. 2). These adaptations likely contribute to E-158's enhanced resistance under high-temperature conditions.

Mechanisms of tolerance to combined heat and ethanol stress in strain E-158

Under dual stress conditions of high temperature (43 °C) and ethanol (3% v/v), using a YP medium with 100 g/L glucose, strain E-158 exhibited significant improvements in glucose consumption and ethanol production, with increases of 82% and 81%, respectively, compared to strain KF-7 [13]. A comparative transcriptomic analysis identified 1646 DEGs in E-158 relative to KF-7, of which 805 were upregulated and 841 were downregulated. All DEGs were subjected to KEGG pathway enrichment analysis (Fig. 1b, Additional file 2: Table S5).

Compared to strain KF-7, strain E-158 exhibited significant upregulation of genes encoding high-affinity glucose transporters (*HXT2*, *HXT6*, *HXT7*, and *HXT8*), which likely enhances glucose uptake into the cell. Concurrently, several genes involved in glycolysis (*EMI2*, *HXX1*, *GLK1*, and *PYK2*) were also upregulated, suggesting an increased flux of glucose through glycolysis. Furthermore, the upregulation of *PDC1*, *ALD2*, *ALD4*, and



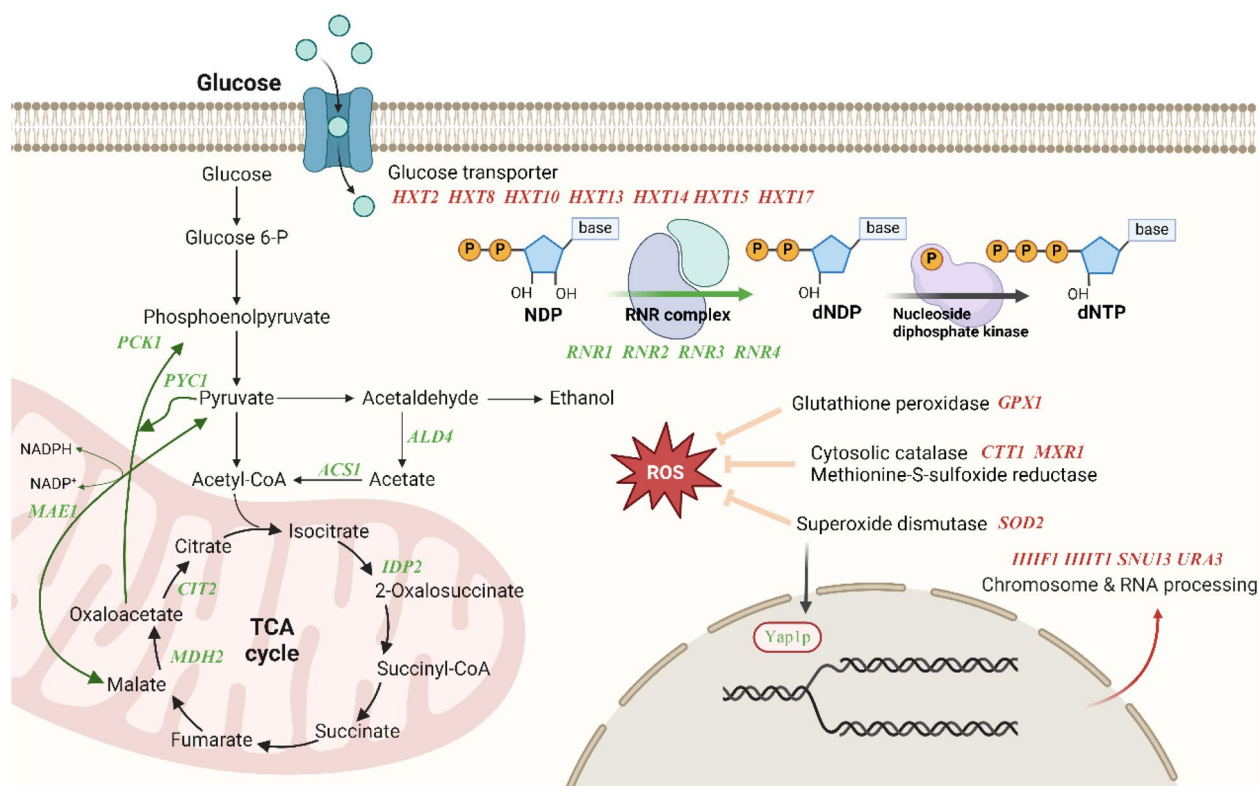


Fig. 2 Transcriptional differences between E-158 and KF-7 under high-temperature stress. Key pathways were identified through KEGG enrichment analysis. Red indicates upregulation; Green indicates downregulation. *ROS* reactive oxygen species, *RNR* ribonucleotide-diphosphate reductase, *NDP* ribonucleotide diphosphates, *dNDP* deoxyribonucleotide diphosphates, *dNTP* deoxynucleoside triphosphate

ALD5 was observed. The increased expression of *PDC1* may lead to higher acetaldehyde production, providing more precursors for ethanol synthesis. The upregulation of *ALD2*, *ALD4*, and *ALD5* not only increases acetic acid production, supplying additional substrates for acetyl-CoA metabolism, but also facilitates NADPH regeneration [25]. In addition, genes involved in glycerol production (*GPD1*, *GPP1*, and *GPP2*) were significantly downregulated, indicating reduced glycerol formation. Consequently, E-158 demonstrated enhanced glucose uptake, increased carbon flux through glycolysis and NADPH regeneration, and reduced glycerol formation. This metabolic reprogramming likely contributes to E-158's superior tolerance to combined heat and ethanol stress.

KEGG enrichment analysis revealed significant involvement in redox processes, particularly those related to glutathione metabolism, ROS response, and cytochrome c function. Genes associated with glutathione (GSH) metabolism (*DUG1*, *GSH1*, and *GSH2*) were all upregulated. GSH is one of the most important antioxidants within cells, effectively handling free radicals and peroxides and restoring protein function [26].

GSH1 and *GSH2* are both involved in GSH biosynthesis, while *DUG1* is involved in GSH catabolism. The upregulation of these genes suggests enhanced GSH metabolic activity in E-158, likely as a mechanism to counteract the combined stress of heat and ethanol. Concurrently, genes associated with ROS scavenging, such as *SOD2* and *MXR1*, also showed increased expression. Superoxide dismutase (encoded by *SOD2*) converts superoxide into hydrogen peroxide, which can activate Yap1p, a key antioxidant TF that plays a signaling role in ethanol tolerance [27]. Peroxisomes are major sites for ROS production and detoxification in yeast cells. In E-158, the upregulation of peroxisome-related genes (*PEX1*, *PEX2*, *PEX6*, *PEX15*, and *PEX19*) indicates strengthened peroxisomal function, further promoting the cell's ability to combat oxidative stress. Impaired peroxisome function has been reported to significantly reduce cellular tolerance to oxidative and heat stress [28]. Moreover, genes participating in the redox process of cytochrome c (*COX1*, *COX2*, *COX3*, *BI2*, *COB*, and *A14*) were downregulated, indicating suppression of the cellular respiratory chain electron transport under dual-stress conditions. Similar to the high-temperature stress condition described above, the

expression of RNR genes (*RNR2*, *RNR3*, and *RNR4*) was significantly reduced in E-158 under combined heat and ethanol stress. This reduction likely decreases DNA replication capacity, conserving reducing equivalents for the stress response. Consequently, E-158 exhibited enhanced glutathione metabolism and ROS clearance activity, activated peroxisomes, suppressed respiration, and minimized the loss of reducing equivalents to maintain intracellular redox homeostasis under combined heat and ethanol stress.

Furthermore, significant enrichment was observed in the ribosomal metabolic pathway, involving 34 DEGs, with 88% showing upregulation. Most of these genes encode proteins for both the large and small ribosomal subunits. This substantial upregulation indicates that under dual-stress conditions of heat and ethanol, strain E-158 might demonstrate robust ribosome synthesis. Consequently, E-158 likely possesses a higher capacity for protein synthesis compared to KF-7. The enhancement of ribosome synthesis and the maintenance or boosting of translational efficiency may serve as adaptive strategies for E-158 to counteract the adverse effects of combined heat and ethanol stress.

In summary, compared to strain KF-7, strain E-158 responds to combined heat (43 °C) and ethanol (3% v/v) stress by enhancing glucose uptake, increasing carbon

flux through glycolysis and NADPH regeneration, boosting antioxidant defenses through activation of the glutathione system and enhanced ROS scavenging, suppressing respiratory activity, and redirecting more reducing equivalents toward antioxidant defenses (Fig. 3). In addition, it promotes protein synthesis capacity. These adaptations likely contribute to E-158's enhanced resistance under combined heat and ethanol stress.

Regulatory networks of E-158 under two stress conditions

Considering the intricate regulatory mechanisms governing tolerance phenotypes, enhancing multi-tolerance by manipulating only a few functional genes presents a significant challenge. Therefore, an in-depth analysis of differentially expressed transcription factors (DETFs) under stress conditions was conducted to identify key transcriptional regulators influencing stress resistance.

This study revealed that under heat stress, 41 TFs showed significant differential expression (Additional file 2: Table S6). By analyzing the regulatory relationships among these 41 DETFs, it was found that 14 DETFs had a regulation ratio exceeding 25%, positioning them at central nodes within the interaction network. *YAP1*, *PDR1*, *MIG1*, and *CRZ1* exhibited over 70% consistency in expression with their targeting DEGs, suggesting that these TFs may play crucial roles in global transcriptional

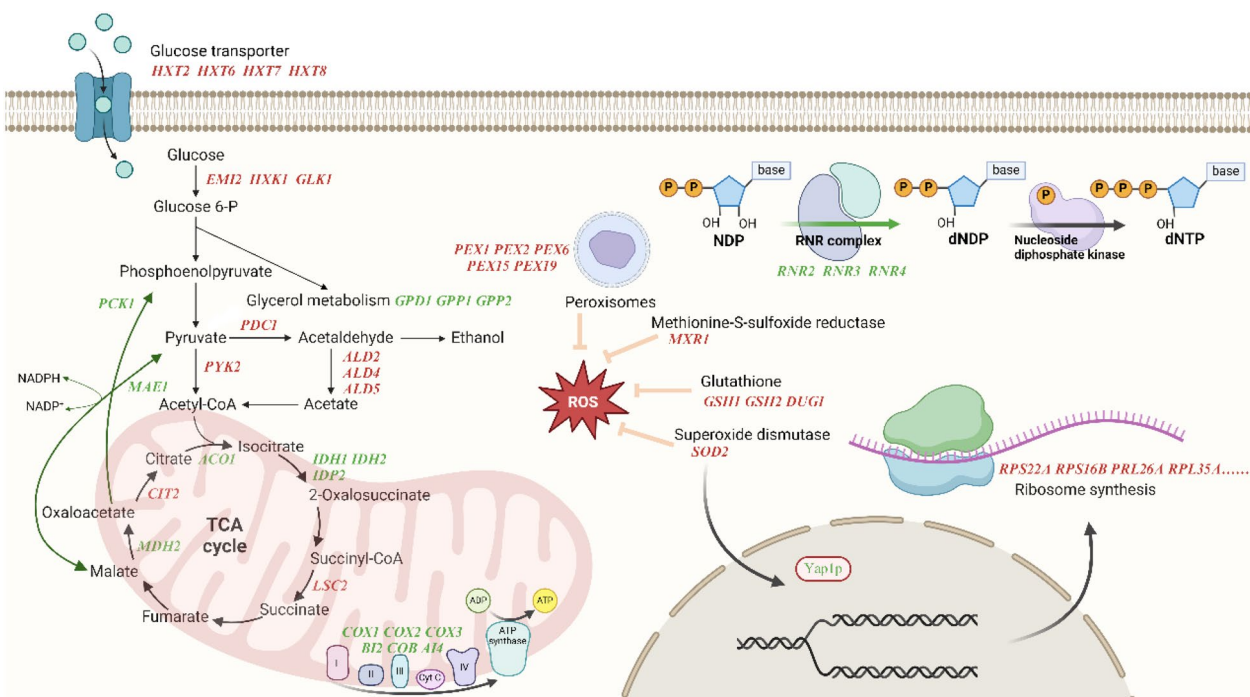


Fig. 3 Transcriptional differences between E-158 and KF-7 under combined high-temperature and ethanol stress. Key pathways were identified through KEGG enrichment analysis. Red indicates upregulation; Green indicates downregulation. ROS reactive oxygen species, RNR ribonucleotide-diphosphate reductase, NDP ribonucleotide diphosphates, dNDP deoxyribonucleotide diphosphates, dNTP deoxynucleoside triphosphate

regulation under heat stress. Mig1p is involved in glucose repression. Previous studies have shown that the deletion of *MIG1* enhances thermotolerance in a laboratory yeast strain, whereas overexpression of *MIG1* benefits thermotolerance in an industrial yeast strain [29]. Moreover, under abiotic stress conditions, elevated intracellular calcium ion concentrations activate the TF Crz1p, which binds to heat shock elements (HSEs) located upstream of heat shock protein genes to promote their transcriptional upregulation [30]. Therefore, it is inferred that Crz1p might play a regulatory role in thermotolerance. Yap1p serves as the master regulator of oxidative stress responses in yeasts, with its activity being induced when cells are exposed to various stress conditions, including oxidative stress, metal ions, ethanol, and different carbon sources [31, 32]. However, prior to this study, no direct association had been established between Yap1p or Pdr1p and thermotolerance. The present study elucidated the regulatory relationships among Yap1p, Pdr1p, Mig1p, and Crz1p, and revealed that they collectively regulate the expression of DEGs related to central carbon metabolism, RNR, and amino acid metabolism (Fig. 4a).

Under combined heat and ethanol stress, 61 TFs exhibited significant differential expression (Additional file 2: Table S7). Among these, 9 DETFs were identified as central nodes in the interaction network (regulatory ratio > 25%). Yap1p, Met32p, Met31p, Met28p, and Cbf1p exhibited a regulatory ratio exceeding 70% over the 61 DETFs. Meanwhile, Yap1p showed over 70% consistency in expression with its targeting DEGs. These TFs may play crucial roles in global transcriptional regulation under combined heat and ethanol stress. Previous studies have shown that Yap1p is associated with ethanol

tolerance [27, 32]. Met28p and Cbf1p are integral components of the Cbf1p–Met4p–Met28p complex, which participates in sulfur metabolism regulation. Met32p and Met31p are involved in the regulation of sulfur amino acid metabolic and the mitotic cell cycle. Besides Yap1p, the direct association of these TFs with thermotolerance or ethanol stress resistance has yet to be established. This study revealed a tight connection among these five TFs, which collectively regulate DEGs involved in central carbon metabolism, cytochrome c oxidase, RNR, glutathione biosynthesis, and methionine metabolism (Fig. 4b).

Identification of key transcription factors relevant to heat and ethanol stress resistance

To identify key TFs active under both stress conditions, 41 DETFs identified under heat stress were compared with 61 DETFs identified under dual heat-ethanol stress, revealing 14 common DETFs: Yap1p, Rph1p, Crz1p, Gis1p, Put3p, Mig1p, Phd1p, Opi1p, Ifh1p, Yjl206c, Dal80p, Uga3p, Ime1p, and Tos8p. Yap1p and Mig1p are known for their roles in ethanol tolerance and thermotolerance [29, 32]. Crz1p activates stress response genes, affecting cell wall synthesis, ionic homeostasis, lipid and sterol metabolism, and glucose metabolism [30, 33]. Rph1p represses autophagy-related genes under nutrient-rich conditions, while Gis1p regulates gene expression during nutrient limitation [34, 35]. Tos8p is linked to chromatin changes during meiosis and cell damage; Ime1p activates early meiotic genes; Phd1p regulates pseudohyphal growth [36]. Opi1p controls phospholipid biosynthesis, and Ifh1p regulates the transcription of ribosomal protein genes [37]. Put3p, Dal80p, and Uga3p

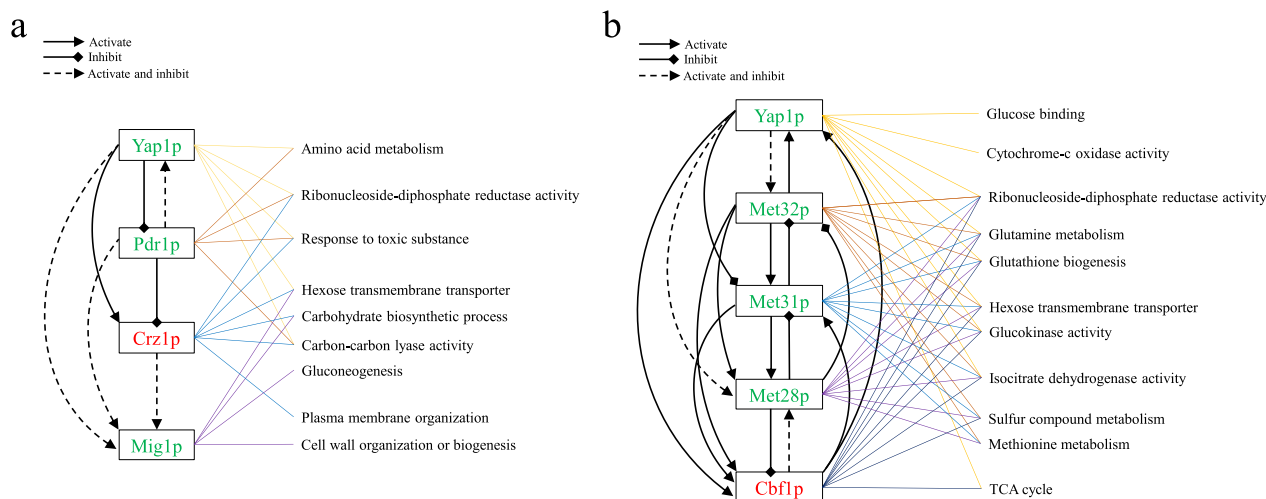


Fig. 4 Regulatory network of E-158 under (a) heat stress and (b) combined heat-ethanol stress. Red indicates upregulation; Green indicates downregulation

regulate nitrogen and amino acid metabolism [38]. Yjl206c is a putative TF with an unknown function. To further investigate their contributions to stress tolerance, each of these 14 TFs was individually overexpressed or deleted in the strain KF-7. Due to the lethality of *IFH1* deletion, 14 overexpression strains and 13 knockout strains were obtained.

The fermentation performance of the engineered strains was first assessed under heat stress at 43 °C, with an initial glucose concentration of 150 g/L (Additional file 1: Figs. S1 and S2). After 24 h of fermentation, strain KF-7 consumed 109.44 ± 4.08 g/L glucose, and produced 45.87 ± 2.32 g/L ethanol with a yield of 0.42 ± 0.03 g/g consumed glucose (Table 3). The impact of TF modifications on thermotolerance was assessed by quantifying improvements in glucose consumption and ethanol production. Among the TF-knockout strains, deletion of

GIS1, *CRZ1*, *YAP1*, and *TOS8* significantly enhanced glucose consumption and ethanol production, with increases exceeding 8% compared to KF-7 (Table 3; Fig. 5a, b). The *GIS1*-knockout strain exhibited the strongest thermotolerance, showing a 13% increase in glucose consumption, a 30% increase in ethanol production, and a 15% higher ethanol yield relative to KF-7 (Table 3). Conversely, deletion of specific TFs, such as *PUT3*, *MIG1*, and *OPI1*, significantly impaired thermotolerance, highlighting their critical roles in the heat stress response. The *PUT3*-knockout strain showed the most pronounced decline in performance, with a 23% reduction in glucose consumption and a 16% decrease in ethanol production compared to KF-7.

Among the TF-overexpression strains, overexpression of *MIG1*, *DAL80*, *TOS8*, *OPI1*, and *CRZ1* resulted in significant increases in ethanol production compared

Table 3 Fermentation performance of engineered strains at 43 °C with 150 g/L glucose

	Consumed glucose (g/L)	Improvement (%)	Ethanol concentration (g/L)	Improvement (%)	Ethanol yield (g/g consumed glucose)
KF-7	109.44 ± 4.08	–	45.87 ± 2.32	–	0.42 ± 0.03
KF7ΔYAP1	119.68 ± 1.96**	9.36	54.18 ± 0.16***	18.12	0.45 ± 0.01
KF7ΔRPH1	113.50 ± 1.62	3.71	46.25 ± 0.13	0.84	0.41 ± 0.01
KF7ΔCRZ1	120.47 ± 3.46**	10.07	56.17 ± 0.80***	22.46	0.47 ± 0.01*
KF7ΔGIS1	123.93 ± 1.59**	13.24	59.99 ± 0.66****	30.79	0.48 ± 0.01**
KF7ΔPUT3	84.13 ± 0.27****	– 23.13	38.24 ± 2.09**	– 16.63	0.45 ± 0.03
KF7ΔMIG1	93.95 ± 1.74***	– 14.15	40.36 ± 0.42**	– 11.99	0.43 ± 0.01
KF7ΔPHD1	108.11 ± 1.67	– 1.21	42.96 ± 4.56	– 6.33	0.40 ± 0.04
KF7ΔOPI1	99.01 ± 0.08**	– 9.53	43.90 ± 0.86	– 4.29	0.44 ± 0.01
KF7ΔYJL206C	108.07 ± 3.15	– 1.25	46.61 ± 2.85	1.62	0.43 ± 0.03
KF7ΔDAL80	112.95 ± 0.64	3.21	47.38 ± 0.99	3.30	0.42 ± 0.01
KF7ΔUGA3	106.96 ± 6.06	– 2.26	45.50 ± 2.57	– 0.80	0.43 ± 0.01
KF7ΔIME1	100.57 ± 3.31*	– 8.10	48.89 ± 0.30	6.59	0.49 ± 0.02*
KF7ΔTOS8	118.50 ± 1.58*	8.28	49.75 ± 1.89	8.47	0.42 ± 0.02
KF7YAP1	94.51 ± 2.17**	– 13.64	39.66 ± 0.59**	– 13.54	0.42 ± 0.01
KF7RPH1	108.53 ± 0.67	– 0.83	43.29 ± 1.30	– 5.63	0.40 ± 0.01
KF7CRZ1	110.02 ± 2.33	0.53	50.26 ± 1.22*	9.58	0.46 ± 0.01
KF7GIS1	92.76 ± 0.03***	– 15.24	43.53 ± 0.38	– 5.10	0.47 ± 0.01*
KF7PUT3	101.38 ± 1.34*	– 7.37	42.38 ± 0.05	– 7.61	0.42 ± 0.01
KF7MIG1	124.04 ± 2.86**	13.35	54.31 ± 1.29**	18.41	0.44 ± 0.01
KF7PHD1	87.11 ± 3.90***	– 20.41	37.64 ± 0.11***	– 17.95	0.43 ± 0.02
KF7OPI1	121.41 ± 0.58**	10.94	51.24 ± 0.11**	11.72	0.42 ± 0.01
KF7YJL206C	89.87 ± 2.81***	– 17.88	40.69 ± 2.78*	– 11.30	0.45 ± 0.02
KF7DAL80	124.33 ± 1.35***	13.61	53.51 ± 0.40**	16.67	0.43 ± 0.01
KF7UGA3	113.59 ± 2.77	3.79	48.14 ± 1.74	4.96	0.42 ± 0.01
KF7IME1	101.70 ± 0.92*	– 7.08	46.64 ± 0.71	1.69	0.46 ± 0.01
KF7TOS8	118.46 ± 2.88*	8.24	51.44 ± 1.90*	12.15	0.43 ± 0.01
KF7IFH1	111.42 ± 7.19	1.81	47.16 ± 3.31	2.82	0.42 ± 0.01

All data were calculated based on 24 h of fermentation. Values indicate mean ± standard deviation of three biological replications. Statistical significance was determined using an independent samples *t* test. Difference is indicated as significant (**p* < 0.05, ***p* < 0.01, ****p* < 0.001, and *****p* < 0.0001) when compared to the control strain KF-7

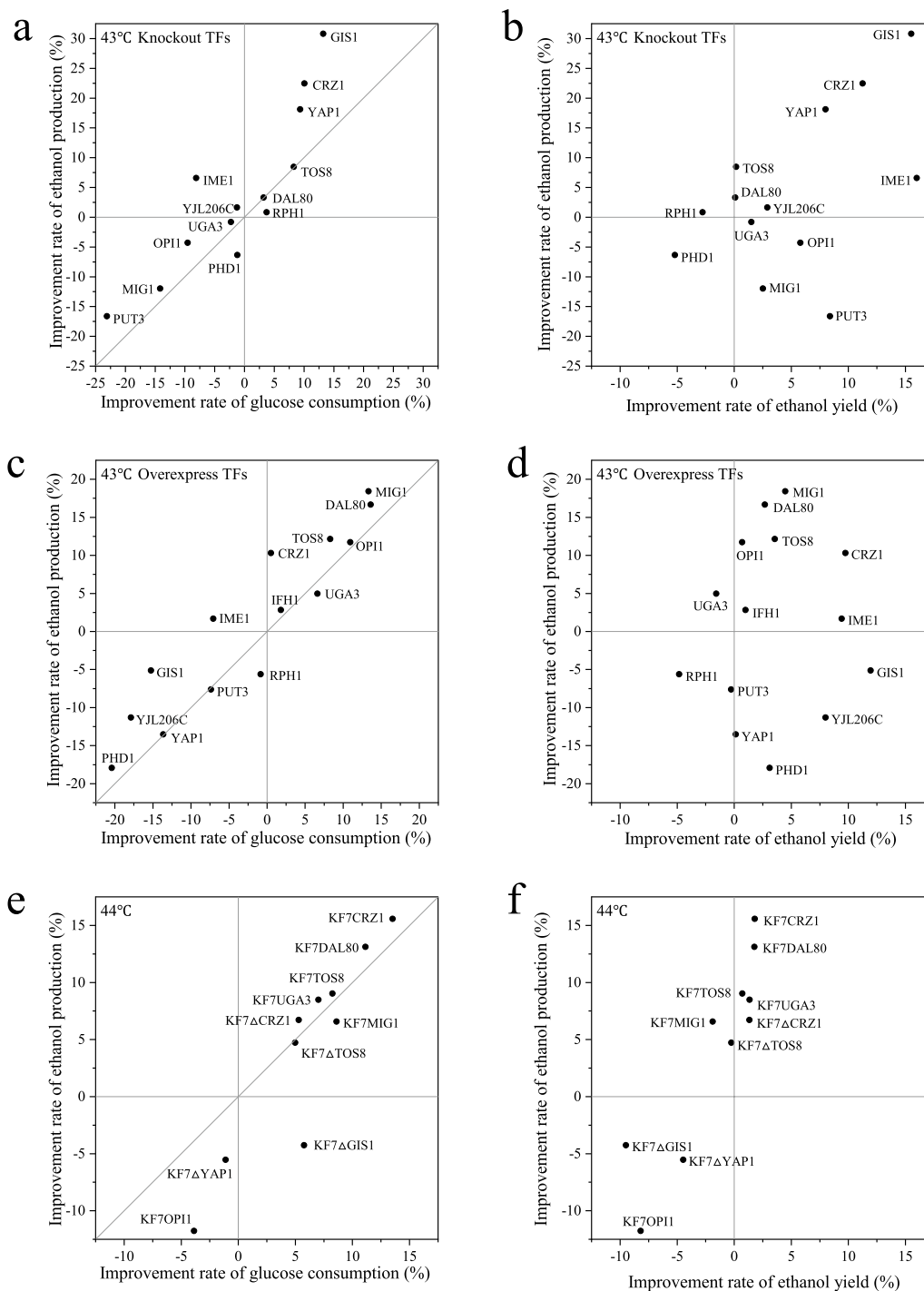


Fig. 5 Contribution of TFs deletion (**a, b**) and overexpression (**c, d**) to thermotolerance at 43 °C after 24 h fermentation. Impact of TFs engineering on heat tolerance at 44 °C (**e, f**) after 48 h fermentation

to KF-7 (Table 3; Fig. 5c, d). The *DAL80* and *MIG1* overexpression strains showed substantial improvements, both exhibiting 13% increases in glucose consumption and more than 16% increases in ethanol production compared to KF-7 (Table 3). However, the overexpression of

TFs including *YAP1*, *GIS1*, *PUT3*, *PHD1*, *YJL206C*, and *IME1* led to significantly reduced thermotolerance. The *PHD1*-overexpression strain exhibited the worst tolerance, with a 20% decrease in glucose consumption and an 18% decrease in ethanol production compared to

KF-7. Overall, knocking out *YAP1* and *GIS1* enhanced thermotolerance, while their overexpression reduced it. Conversely, *MIG1* and *OPI1* showed opposite effects: their knockouts impaired thermotolerance, whereas their overexpression improved it. Both knockouts and overexpression of *CRZ1* and *TOS8* enhanced thermotolerance. In contrast, modifications to *PUT3*, *PHD1*, and *YJL206C* were detrimental to thermotolerance.

To further assess the strains with improved thermotolerance at 43 °C, fermentation at 44 °C was carried out using an initial glucose concentration of 150 g/L (Additional file 1: Fig. S3). After 48 h of fermentation, KF-7 consumed 87.83 ± 4.09 g/L glucose, and produced 38.29 ± 1.11 g/L ethanol, with an ethanol yield of 0.44 ± 0.01 g/g consumed glucose (Table 4). Similar to the observations at 43 °C, both overexpression and knockout of *CRZ1* and *TOS8* enhanced thermotolerance (Table 4, Fig. 5e, f). In addition, overexpression of *MIG1*, *DAL80*, and *UGA3* also enhanced thermotolerance. In contrast to the observations at 43 °C, knocking out *YAP1* and *GIS1*, as well as overexpression of *OPI1*, resulted in decreased thermotolerance. Among all strains, the *DAL80* overexpression strain (KF7DAL80) and the *CRZ1* overexpression strain (KF7CRZ1) exhibited the best thermotolerance. Specifically, KF7DAL80 showed a 10% increase in glucose consumption and a 12% increase in ethanol production, while KF7CRZ1 showed a 12% increase in glucose consumption and a 15% increase in ethanol production, both compared to KF-7.

To evaluate their tolerance to multiple stresses, KF7DAL80 and KF7CRZ1 were fermented under combined heat (43 °C) and ethanol (3% v/v) stress, with an initial glucose concentration of 100 g/L (Fig. 6). The combined heat and ethanol stress exerted greater pressure on

the strains compared to heat stress alone. After 48 h of fermentation, KF-7 consumed only 25.87 ± 1.25 g/L glucose and produced 9.07 ± 0.80 g/L ethanol, with an ethanol yield of 0.35 ± 0.02 g/g (Table 5). Compared to KF-7, KF7CRZ1 demonstrated increases of 44% in glucose consumption, 77% in ethanol production, and 22% in ethanol yield. In contrast, KF7DAL80 showed increases of 67% in glucose consumption, 116% in ethanol production, and 28% in ethanol yield. The multi-tolerant strain E-158 consumed 37.03 ± 1.44 g/L glucose and produced 16.36 ± 2.02 g/L ethanol with a yield of 0.44 ± 0.06 g/g under these conditions (Table 5). Compared to E-158, KF7CRZ1 showed nearly identical fermentation performance, while KF7DAL80 exhibited superior fermentation performance. These results suggest that both *CRZ1* and *DAL80* play crucial roles in enhancing E-158's tolerance to combined heat and ethanol stress.

Discussion

Currently, numerous studies have employed omics approaches to investigate the mechanisms by which *S. cerevisiae* strains respond to high temperatures, encompassing dynamic transcriptional responses to short-term heat stress [39, 40], as well as adaptation mechanisms under long-term heat stress [41, 42]. However, the highest reported temperature tolerance of existing thermotolerant strains does not exceed 42 °C [43, 44]. In contrast, the multi-tolerant strain E-158 utilized in this study exhibits remarkable performance under 44 °C heat stress. Comparative transcriptomic analysis between E-158 and its parental strain KF-7 at 44 °C elucidated the unique thermotolerance mechanisms inherent to E-158. In E-158, the activation of ROS scavenging activity and glutathione metabolism

Table 4 Fermentation performance of engineered strains at 44 °C with 150 g/L glucose

	Consumed glucose (g/L)	Improvement (%)	Ethanol concentration (g/L)	Improvement (%)	Ethanol yield (g/g consumed glucose)
KF-7	87.83 ± 4.09	–	38.29 ± 1.11	–	0.44 ± 0.01
KF7ΔYAP1	86.15 ± 1.03	– 1.91	35.99 ± 1.25	– 6.01	0.42 ± 0.01
KF7ΔCRZ1	91.74 ± 3.17	4.45	40.66 ± 1.56	6.19	0.44 ± 0.01
KF7ΔGIS1	92.14 ± 1.10	4.91	36.48 ± 0.54	– 4.74	0.40 ± 0.01**
KF7ΔTOS8	91.47 ± 1.74	4.14	39.91 ± 0.95	4.21	0.44 ± 0.01
KF7CRZ1	98.90 ± 1.49**	12.60	44.04 ± 1.20***	14.99	0.45 ± 0.01
KF7MIG1	94.62 ± 0.05*	7.73	40.61 ± 0.28*	6.03	0.43 ± 0.01
KF7OPI1	83.73 ± 0.77	– 4.66	33.62 ± 0.86**	– 12.21	0.40 ± 0.01*
KF7DAL80	96.83 ± 1.21*	10.25	43.10 ± 0.83**	12.56	0.45 ± 0.01
KF7UGA3	93.24 ± 1.72	6.17	41.33 ± 0.31**	7.94	0.44 ± 0.01
KF7TOS8	94.31 ± 0.76	7.38	41.55 ± 0.52**	8.49	0.44 ± 0.01

All data were calculated based on 48 h of fermentation. Values indicate mean ± standard deviation of three biological replications. Statistical significance was determined using an independent samples t test. Difference is indicated as significant (* $p < 0.05$, ** $p < 0.01$, and *** $p < 0.001$) when compared to the control strain KF-7

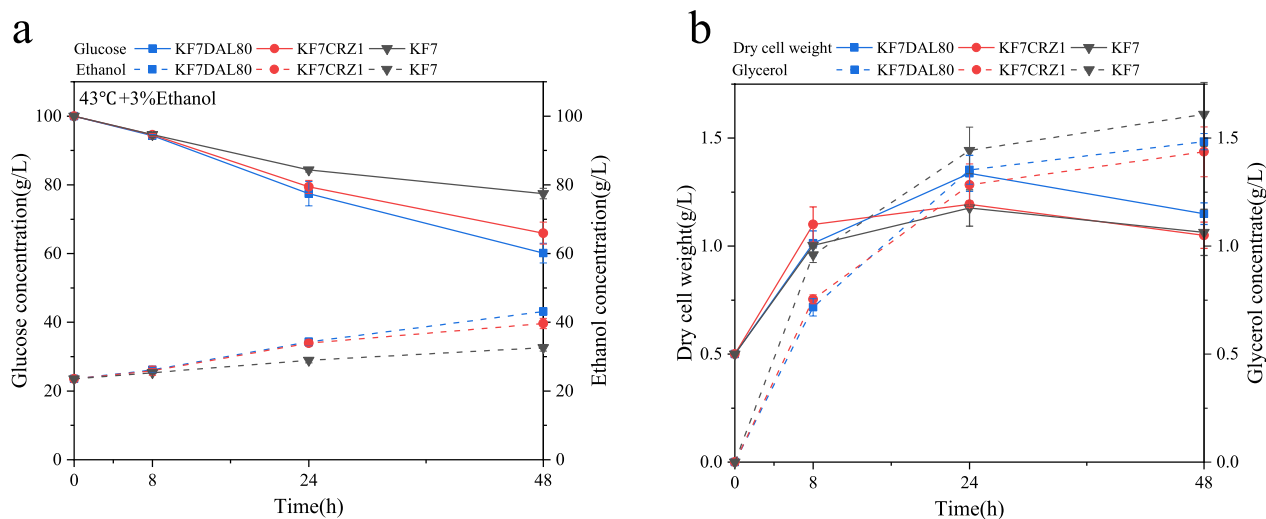


Fig. 6 Fermentation performance of strains under combined 43 °C and 3% (v/v) ethanol stress. **a** Glucose and ethanol concentrations. **b** Dry cell weight and glycerol concentration

Table 5 Fermentation performance of strains under combined heat and ethanol stress with 100 g/L glucose

Strains	Consumed glucose (g/L)	Improvement (%)	Ethanol concentration (g/L)	Improvement (%)	Ethanol yield (g/g consumed glucose)
KF-7	25.87 ± 1.25	–	9.07 ± 0.80	–	0.35 ± 0.02
KF7CRZ1	37.39 ± 2.61**	44.53	16.10 ± 1.22**	77.54	0.43 ± 0.01**
KF7DAL80	43.20 ± 2.34***#	67.00	19.61 ± 0.90***	116.32	0.45 ± 0.01**
E-158	37.03 ± 1.44	43.13	16.36 ± 2.02	80.40	0.44 ± 0.06

All data were calculated based on 48 h of fermentation. Values indicate mean ± standard deviation of three biological replications. Statistical significance was determined using an independent samples *t* test. Difference is indicated as significant (* $p < 0.05$, ** $p < 0.01$, and *** $p < 0.001$) when compared to the control strain KF-7. Difference is indicated as significant (# $p < 0.05$) when compared to the control strain E-158

aligns with general heat response mechanisms; however, it does not involve the typical activation of heat shock proteins or trehalose accumulation under heat stress [43, 45, 46]. The unique upregulation of glucose uptake genes and downregulation of acetate production-related genes in E-158 may contribute to enhanced glucose metabolism and ethanol production under heat stress.

The modification of several key TFs identified under 44 °C heat stress significantly improved the thermotolerance of KF-7, providing crucial gene targets for engineering robust thermotolerant strains. For instance, individually deleting *YAP1*, *CRZ1*, *GIS1*, and *TOS8* or overexpressing *CRZ1*, *MIG1*, *OPI1*, *DAL80*, *TOS8*, and *UGA3*, resulted in enhanced thermotolerance at 43 °C. When the temperature is elevated to 44 °C, individual knockouts of *CRZ1* and *TOS8*, as well as overexpression of *CRZ1*, *TOS8*, *MIG1*, *DAL80*, and *UGA3*, contribute to enhanced cellular thermotolerance. These findings indicate that even a one-degree increase in temperature can

lead to significant differences in the mechanisms regulating thermotolerance.

Yap1p is a key TF that plays a critical role in responding to oxidative stress. Studies have shown that overexpression of *YAP1* can enhance the yeast's tolerance to various stresses, including HMF, ROS, and ethanol [32, 47, 48]. Conversely, knocking out *YAP1* leads to increased sensitivity to oxidative stress [49, 50]. However, in this study, *YAP1* was downregulated in E-158 under both stress conditions. In addition, *YAP1* knockout strain exhibited improved fermentation performance at 43 °C, but showed reduced performance at 44 °C. These results suggest that the contribution of Yap1p to stress resistance may be influenced by multiple factors, such as the type of stress, the genetic background of the strains, and the severity of the stress.

To date, no studies have investigated the relationship between Opi1p, Uga3p, Gis1p, Dal80p and heat tolerance. Opi1p is a regulator of phospholipid biosynthesis genes and plays a key role in coordinating membrane

biogenesis and fat storage. Previous research has demonstrated that knocking out *OPI1* leads to increased fatty alcohol synthesis and enhanced resistance to lactic acid [51, 52]. Uga3p is a TF involved in the induction of γ -aminobutyric acid (GABA) metabolism genes. Gutmann et al. [53] reported that overexpression of *UGA3* improves yeast tolerance to lignocellulosic hydrolysates. Gis1p is essential for gene expression during nutrient limitation, and its deletion results in significant growth defects [54]. Dal80p regulates genes participating in the metabolism of glutamine, glutamate, proline, and urea [55]. The roles of these TFs in thermotolerance are not clearly linked to their known functions. This study provides the first evidence that Opi1p, Uga3p, Gis1p, and Dal80p are associated with heat stress tolerance in *S. cerevisiae*.

Consistent with our previous findings, overexpression of *CRZ1* and knockout of *TOS8* were shown to enhance thermotolerance [14]. Previous studies have shown that overexpression of *CRZ1* in *S. cerevisiae* enhanced resistance to high salt and low temperature [33, 56]. In this study, we further demonstrate that knockout of *CRZ1* and overexpression of *TOS8* also improve the thermotolerance of the strain. These results suggest that Crz1p and Tos8p may possess dual regulatory roles within the transcriptional regulation network, necessitating systematic investigation in future studies.

Under high temperatures, cells exhibit increased sensitivity to ethanol, and the mechanisms of thermotolerance and ethanol tolerance in *S. cerevisiae* are interdependent [57]. Most studies have primarily focused on single stress conditions, whereas the combination of heat and ethanol stress remains relatively underexplored. The present study elucidates the tolerance mechanisms of the multi-tolerant strain E-158 under combined heat and ethanol stress, providing new insights.

Similar to the response under heat stress alone, E-158 demonstrated enhanced ROS scavenging activity, glutathione metabolism, and glucose uptake under combined heat and ethanol stress. However, E-158 also exhibited enhanced ribosome synthesis and acetate production, as well as suppressed glycerol synthesis. This result supports previous findings that ribosomal protein genes are upregulated in ethanol-tolerant strains under ethanol stress [58]. Under heat stress alone, acetate production genes in E-158 were downregulated, potentially reducing acetate accumulation. In contrast, under dual heat-ethanol stress, these genes were upregulated to promote NADPH generation. Both mechanisms are beneficial for enhancing cellular stress resistance. Overproduction of glycerol has been reported to play a crucial role in improving thermotolerance, osmotolerance, and ethanol tolerance [41]. However, under heat-ethanol

stress, glycerol production genes in E-158 were downregulated, suggesting that E-158 may resist stress through mechanisms independent of glycerol synthesis. In summary, the tolerance mechanisms of E-158 under dual heat and ethanol stress show both shared features with those under heat stress alone and distinct characteristics unique to the combined stress conditions.

Overexpression of *DAL80* and *CRZ1* significantly enhanced the tolerance of KF-7 to combined heat and ethanol stress. Notably, the recombined strain KF7CRZ1 displayed fermentation performance nearly identical to that of E-158, whereas KF7DAL80 exhibited significantly enhanced fermentation performance, surpassing that of E-158. These results not only highlight the critical roles of Crz1p and Dal80p in regulating both heat stress and dual heat-ethanol stress tolerance in *S. cerevisiae*, but also illustrate the effectiveness of reverse metabolic engineering in identifying key TFs from multi-tolerant strains. Considering the functional differences of key TFs under heat stress and dual heat-ethanol stress, a further evaluation of the remaining 12 key TFs for their contributions to dual heat-ethanol stress tolerance is warranted.

Conclusions

This study employed comparative transcriptomics to investigate the tolerance mechanisms of the multi-tolerant *S. cerevisiae* strain E-158 under heat stress and combined heat-ethanol stress. The results indicated that key response pathways include transmembrane transport, central carbon metabolism, antioxidant defense, and ribosome metabolism. By conducting overexpression and knockout experiments on the 14 common DETFs, a series of important targets were identified that significantly improve tolerance to both high temperatures and ethanol stress. Notably, the overexpression of *DAL80* and *CRZ1* significantly enhanced dual tolerance in *S. cerevisiae*. This study is the first to reveal that Dal80p plays a role in heat and ethanol stress tolerance in *S. cerevisiae*. The findings provide theoretical guidance and identifies critical TF targets for constructing robust strains suitable for bioethanol production.

Abbreviations

<i>S. cerevisiae</i>	<i>Saccharomyces cerevisiae</i>
ROS	Reactive oxygen species
TCA cycle	Tricarboxylic acid cycle
TFs	Transcription factors
SSF	Simultaneous saccharification and fermentation
UV-DES	Ultraviolet-diethyl sulfate
ARTP	Atmospheric and room temperature plasma
NCBI	National Center for Biotechnology Information
SGD	<i>Saccharomyces Genome Database</i>
TPM	Transcripts per million reads
FDR	False discovery rate
FC	Fold change
DEGs	Differentially expressed genes
DETFs	Differentially expressed transcription factors

gRNA	Guide RNA
DCW	Dry cell weight
HPLC	High-performance liquid chromatography
GC	Gas chromatography
KEGG	Kyoto Encyclopedia of Genes and Genomes
RNR	Ribonucleotide–diphosphate reductase
NDPs	Ribonucleotide diphosphates
dNDPs	Deoxyribonucleotide diphosphates
NADPH	Nicotinamide adenine dinucleotide phosphate
HSEs	Heat shock elements

Supplementary Information

The online version contains supplementary material available at <https://doi.org/10.1186/s13068-025-02653-2>.

Supplementary Material 1.
Supplementary Material 2.

Acknowledgements

Not applicable.

Author contributions

RR C and L W conducted experiments. RR C and CY X analyzed data and wrote the main manuscript. CY X and XX J provided technical assistance during the experiment and data analysis. YQ T designed the study, revised the manuscript, and acquired financial support. All authors read and approved of the final manuscript.

Funding

This study was financially supported by the National Key R&D Program of China (2022YFE0108500).

Availability of data and materials

The dataset(s) used and/or analyzed during the current study are available from the corresponding author on reasonable request. The raw sequence data can be accessed in the National Center for Biotechnology Information (<http://www.ncbi.nlm.nih.gov/>) through the accession number PRJNA642097.

Declarations

Ethics approval and consent to participate

Not applicable.

Consent for publication

Not applicable.

Competing interests

The authors declare no competing interests.

Author details

¹College of Architecture and Environment, Sichuan University, Chengdu 610065, Sichuan, China. ²Sichuan Environmental Protection Key Laboratory of Organic Wastes Valorization, Chengdu 610065, Sichuan, China. ³Engineering Research Center of Alternative Energy Materials and Devices, Ministry of Education, Chengdu 610065, Sichuan, China.

Received: 20 January 2025 Accepted: 25 April 2025

Published online: 03 May 2025

References

- Sarkar N, Ghosh SK, Bannerjee S, Aikat K. Bioethanol production from agricultural wastes: an overview. *Renew Energ.* 2012;37:19–27.
- Jhariya U, Dafale NA, Srivastava S, Bhende RS, Kapley A, Purohit HJ. Understanding ethanol tolerance mechanism in *Saccharomyces cerevisiae* to enhance the bioethanol production: current and future prospects. *Bioenerg Res.* 2021;14:670–88.
- Afedzi AEK, Parakulsuksatid P. Recent advances in process modifications of simultaneous saccharification and fermentation (SSF) of lignocellulosic biomass for bioethanol production. *Biocatal Agr Biotech.* 2023;54:102961.
- Xu Y, Li J, Zhang M, Wang D. Modified simultaneous saccharification and fermentation to enhance bioethanol titers and yields. *Fuel.* 2018;215:647–54.
- Bertacchi S, Jayaprakash P, Morrissey JP, Branduardi P. Interdependence between lignocellulosic biomasses, enzymatic hydrolysis and yeast cell factories in biorefineries. *Microb Biotechnol.* 2022;15:985–95.
- Siriwong T, Laimheeriwa B, Aini UN, Cahyanto MN, Reungsang A, Salakam A. Cold hydrolysis of cassava pulp and its use in simultaneous saccharification and fermentation (SSF) process for ethanol fermentation. *J Biotechnol.* 2019;292:57–63.
- Sharma J, Kumar V, Prasad R, Gaur NA. Engineering of *Saccharomyces cerevisiae* as a consolidated bioprocessing host to produce cellulosic ethanol: recent advancements and current challenges. *Biotechnol Adv.* 2022;56:107925.
- da Silva FF, de Souza ÉS, Carneiro LM, Alves Silva JP, de Souza JVB, da Silva BJ. Current ethanol production requirements for the yeast *Saccharomyces cerevisiae*. *Int J Microbiol.* 2022;2022:7878830.
- Pandey AK, Kumar M, Kumari S, Kumari P, Yusuf F, Jakeer S, Naz S, Chandna P, Bhatnagar I, Gaur NA. Evaluation of divergent yeast genera for fermentation-associated stresses and identification of a robust sugarcane distillery waste isolate *Saccharomyces cerevisiae* NGY10 for lignocellulosic ethanol production in SHF and SSF. *Biotechnol Biofuels.* 2019;12:40.
- Auesukaree C, Koedrith P, Saenpayavai P, Asvarak T, Benjaphokee S, Sugiyama M, Kaneko Y, Harashima S, Boonchird C. Characterization and gene expression profiles of thermotolerant *Saccharomyces cerevisiae* isolates from Thai fruits. *J Biosci Bioeng.* 2012;114:144–9.
- Yang T, Zhang S, Li L, Tian J, Li X, Pan Y. Screening and transcriptomic analysis of the ethanol-tolerant mutant *Saccharomyces cerevisiae* YN81 for high-gravity brewing. *Front Microbiol.* 2022;13:976321.
- Gan Y, Qi X, Lin Y, Guo Y, Zhang Y, Wang Q. A hierarchical transcriptional regulatory network required for long-term thermal stress tolerance in an industrial *Saccharomyces cerevisiae* strain. *Front Bioeng Biotechnol.* 2021;9:826238.
- Wang L, Li B, Wang SP, Xia ZY, Gou M, Tang YQ. Improving multiple stress-tolerance of a flocculating industrial *Saccharomyces cerevisiae* strain by random mutagenesis and hybridization. *Process Biochem.* 2021;102:275–85.
- Wang L, Li B, Su RR, Wang SP, Xia ZY, Xie CY, Tang YQ. Screening novel genes by a comprehensive strategy to construct multiple stress-tolerant industrial *Saccharomyces cerevisiae* with prominent bioethanol production. *Biotechnol Biofuels Bioprod.* 2022;15:11.
- Kida K, Kume K, Morimura S, Sonoda Y. Repeated-batch fermentation process using a thermotolerant flocculating yeast constructed by protoplast fusion. *J Ferment Bioeng.* 1992;74:169–73.
- Concordet JP, Haeussler M. CRISPOR: intuitive guide selection for CRISPR/Cas9 genome editing experiments and screens. *Nucleic Acids Res.* 2018;46:242–5.
- Li B, Wang L, Wu YJ, Xia ZY, Yang BX, Tang YQ. Improving acetic acid and furfural resistance of xylose-fermenting *Saccharomyces cerevisiae* strains by regulating novel transcription factors revealed via comparative transcriptomic analysis. *Appl Environ Microb.* 2021;87:e00158-e221.
- Mans R, van Rossum HM, Wijsman M, Backx A, Kuijpers NGA, van den Broek M, Daran-Lapujade P, Pronk JT, van Maris AJA, Daran JMG. CRISPR/Cas9: a molecular Swiss army knife for simultaneous introduction of multiple genetic modifications in *Saccharomyces cerevisiae*. *FEMS Yeast Res.* 2015;15:004.
- Xie CY, Yang BX, Wu YJ, Xia ZY, Gou M, Sun ZY, Tang YQ. Construction of industrial xylose-fermenting *Saccharomyces cerevisiae* strains through combined approaches. *Process Biochem.* 2020;96:80–9.
- Zhang X, Nijland JG, Driessen AJM. Combined roles of exporters in acetic acid tolerance in *Saccharomyces cerevisiae*. *Biotechnol Biofuels Bioprod.* 2022;15:67.
- Dziadkowiec D, Krasowska A, Liebner A, Sigler K. Protective role of mitochondrial superoxide dismutase against high osmolarity, heat and

- metalloid stress in *Saccharomyces cerevisiae*. *Folia Microbiol (Praha)*. 2007;52:120–6.
22. Rona G, Herdeiro R, Mathias CJ, Torres FA, Pereira MD, Eleuthero E. *CTT1* overexpression increases life span of calorie-restricted *Saccharomyces cerevisiae* deficient in Sod1. *Biogerontology*. 2015;16:343–51.
 23. Jung KW, Kwon S, Jung JH, Bahn YS. Essential roles of ribonucleotide reductases under DNA damage and replication stresses in *Cryptococcus neoformans*. *Microbiol Spectr*. 2022;10: e0104422.
 24. Greene BL, Kang G, Cui C, Bennati M, Nocera DG, Drennan CL, Stubbe J. Ribonucleotide reductases: structure, chemistry, and metabolism suggest new therapeutic targets. *Annu Rev Biochem*. 2020;89:45–75.
 25. Lei C, Guo X, Zhang M, Zhou X, Ding N, Ren J, et al. Regulating the metabolic flux of pyruvate dehydrogenase bypass to enhance lipid production in *Saccharomyces cerevisiae*. *Commun Biol*. 2024;7:1399.
 26. Santos LO, Silva PGP, Lemos Junior WJF, de Oliveira VS, Anschau A. Glutathione production by *Saccharomyces cerevisiae*: current state and perspectives. *Appl Microbiol Biotechnol*. 2022;106:1879–94.
 27. Zyrina AN, Smirnova EA, Markova OV, Severin FF, Knorre DA. Mitochondrial superoxide dismutase and Yap1p act as a signaling module contributing to ethanol tolerance of the yeast *Saccharomyces cerevisiae*. *Appl Environ Microb*. 2017;83:e02759–e2816.
 28. Lin NX, He RZ, Xu Y, Yu XW. Augmented peroxisomal ROS buffering capacity renders oxidative and thermal stress cross-tolerance in yeast. *Microb Cell Fact*. 2021;20:131.
 29. Xiao W, Duan X, Lin Y, Cao Q, Li S, Guo Y, et al. Distinct proteome remodeling of industrial *Saccharomyces cerevisiae* in response to prolonged thermal stress or transient heat shock. *J Proteome Res*. 2018;17:1812–25.
 30. Roy A, Tamuli R. Heat shock proteins and the calcineurin-crz1 signaling regulate stress responses in fungi. *Arch Microbiol*. 2022;204:240.
 31. Samakkarn W, Ratanakhanokchai K, Soontornngun N. Reprogramming of the ethanol stress response in *Saccharomyces cerevisiae* by the transcription factor Znf1 and its effect on the biosynthesis of glycerol and ethanol. *Appl Environ Microbiol*. 2021;87: e0058821.
 32. Bleoanca I, Silva ARC, Pimentel C, Rodrigues-Pousada C, Menezes RD. Relationship between ethanol and oxidative stress in laboratory and brewing yeast strains. *J Biosci Bioeng*. 2013;116:697–705.
 33. Zuo F, Wu Y, Sun Y, Xie C, Tang Y. Mechanism of enhanced salt tolerance in *Saccharomyces cerevisiae* by *CRZ1* overexpression. *Sci Rep*. 2024;14:22875.
 34. Shu WJ, Chen RF, Yin ZH, Li F, Zhang H, Du HN. Rph1 coordinates transcription of ribosomal protein genes and ribosomal RNAs to control cell growth under nutrient stress conditions. *Nucleic Acids Res*. 2020;48:8360–73.
 35. Mota MN, Martins LC, Sa-Correia I. The identification of genetic determinants of methanol tolerance in yeast suggests differences in methanol and ethanol toxicity mechanisms and candidates for improved methanol tolerance engineering. *J Fungi (Basel)*. 2021;7:90.
 36. Pothoulakis G, Ellis T. Synthetic gene regulation for independent external induction of the *Saccharomyces cerevisiae* pseudohyphal growth phenotype. *Commun Biol*. 2018;1:7.
 37. Guo X, Zhao B, Zhou X, Ni X, Lu D, Chen T, Chen Y, Xiao D. Increased RNA production in *Saccharomyces cerevisiae* by simultaneously overexpressing *FHL1*, *IFH1*, and *SSF2* and deleting *HRP1*. *Appl Microbiol Biotechnol*. 2020;104:7901–13.
 38. Turner SA, Ma Q, Ola M, Martinez de San Vicente K, Butler G. Dal81 regulates expression of arginine metabolism genes in *Candida parapsilosis*. *mSphere*. 2018; 3.
 39. Puig-Castellví F, Alfonso I, Piña B, Tauler R. A quantitative 1H NMR approach for evaluating the metabolic response of *Saccharomyces cerevisiae* to mild heat stress. *Metabolomics*. 2015;11:1612–25.
 40. Verghese J, Abrams J, Wang Y, Morano KA. Biology of the heat shock response and protein chaperones: budding yeast (*Saccharomyces cerevisiae*) as a model system. *Microbiol Mol Biol Rev*. 2012;76:115–58.
 41. Caspeta L, Chen Y, Nielsen J. Thermotolerant yeasts selected by adaptive evolution express heat stress response at 30 °C. *Sci Rep-UK*. 2016;6:27003.
 42. Shui W, Xiong Y, Xiao W, Qi X, Zhang Y, Lin Y, Guo Y, Zhang Z, Wang Q, Ma Y. Understanding the mechanism of thermotolerance distinct from heat shock response through proteomic analysis of industrial strains of *Saccharomyces cerevisiae*. *Mol Cell Proteomics*. 2015;14:1885–97.
 43. Saini P, Beniwal A, Kokkiligadda A, Vij S. Response and tolerance of yeast to changing environmental stress during ethanol fermentation. *Process Biochem*. 2018;72:1–12.
 44. Xu JR, Mehmood MA, Wang L, Ahmad N, Ma HJ. OMICs-based strategies to explore stress tolerance mechanisms of *Saccharomyces cerevisiae* for efficient fuel ethanol production. *Front Energy Res*. 2022; 10.
 45. Deparis Q, Claes A, Foulquié-Moreno MR, Thevelein JM. Engineering tolerance to industrially relevant stress factors in yeast cell factories. *FEMS Yeast Res*. 2017;17:fox036.
 46. Fay JC, Alonso-Del-Real J, Miller JH, Querol A. Divergence in the *Saccharomyces* species' heat shock response is indicative of their thermal tolerance. *Genome Biol Evol*. 2023;15:evad207.
 47. Liu ZL, Ma MG. Pathway-based signature transcriptional profiles as tolerance phenotypes for the adapted industrial yeast *Saccharomyces cerevisiae* resistant to furfural and HMF. *Appl Microbiol Biot*. 2020;104:3473–92.
 48. Bouchez C, Devin A. Mitochondrial biogenesis and mitochondrial reactive oxygen species (ROS): a complex relationship regulated by the cAMP/PKA signaling pathway. *Cells*. 2019;8:287.
 49. Ng CH, Tan SX, Perrone GG, Thorpe GW, Higgins VJ, Dawes IW. Adaptation to hydrogen peroxide in *Saccharomyces cerevisiae*: the role of NADPH-generating systems and the *SKN7* transcription factor. *Free Radic Biol Med*. 2008;44:1131–45.
 50. Gales G, Penninckx M, Block JC, Leroy P. Role of glutathione metabolism status in the definition of some cellular parameters and oxidative stress tolerance of *Saccharomyces cerevisiae* cells growing as biofilms. *FEMS Yeast Res*. 2008;8:667–75.
 51. Covino R, Hummer G, Ernst R. Integrated functions of membrane property sensors and a hidden side of the unfolded protein response. *Mol Cell*. 2018;71:458–67.
 52. Berterame NM, Porro D, Ami D, Branduardi P. Protein aggregation and membrane lipid modifications under lactic acid stress in wild type and *OPI1* deleted *Saccharomyces cerevisiae* strains. *Microb Cell Fact*. 2016;15:39.
 53. Gutmann F, Jann C, Pereira F, Johansson A, Steinmetz LM, Patil KR. CRISPRi screens reveal genes modulating yeast growth in lignocellulose hydrolysate. *Biotechnol Biofuels*. 2021;14:41.
 54. Kawai K, Kanesaki Y, Yoshikawa H, Hirasawa T. Identification of metabolic engineering targets for improving glycerol assimilation ability of *Saccharomyces cerevisiae* based on adaptive laboratory evolution and transcriptome analysis. *J Biosci Bioeng*. 2019;128:162–9.
 55. Wei T, Jiao Z, Hu J, Lou H, Chen Q. Chinese yellow rice wine processing with reduced ethyl carbamate formation by deleting transcriptional regulator Dal80p in *Saccharomyces cerevisiae*. *Molecules*. 2020;25:3580.
 56. Panadero J, Hernández-López MJ, Prieto JA, Rande-Gil F. Overexpression of the calcineurin target *CRZ1* provides freeze tolerance and enhances the fermentative capacity of baker's yeast. *Appl Environ Microbiol*. 2007;73:4824–31.
 57. Riles L, Fay JC. Genetic basis of variation in heat and ethanol tolerance in *Saccharomyces cerevisiae*. G3 (Bethesda, Md). 2019;9:179–88.
 58. Li BZ, Cheng JS, Ding MZ, Yuan YJ. Transcriptome analysis of differential responses of diploid and haploid yeast to ethanol stress. *J Biotechnol*. 2010;148:194–203.

Publisher's Note

Springer Nature remains neutral with regard to jurisdictional claims in published maps and institutional affiliations.